Journal of Information Systems Engineering and Management
2025, 10(31s)
e-ISSN: 2468-4376
https://www.jisem-journal.com/

Research Article

Droop and Adaptive Virtual Inertia Controller of PV Inverters for Frequency Regulation in Microgrid

Srinivas Cheera [1], Dr T. Murali Krishna [2], Prof. B Mangu [3]
[1,3] *Department of Electrical Engineering, University College of Engineering(A), Osmania University, Hyderabad, Telangana, India*
[2] *Department of Electrical and Electronics Engineering, CBIT, Hyderabad, Telangana, India*

ARTICLE INFO

Received: 30 Dec 2024

Revised: 12 Feb 2025

Accepted: 26 Feb 2025

ABSTRACT

In this renewable energy era, the power from the solar PV arrays increasing. The world is reducing the power from fossil fuels to reducing carbon emissions. Hence the concept of microgrid with support form solar PV power and energy storage is significant. A local microgrid can reduce the losses as well as use effectively the generated power. In this paper, the two PV inverters are operated in parallel, with support from the battery. PV inverters are used to supply the critical load in a microgrid environment. The control algorithm of the PV inverters includes the implementation of virtual synchronous generator concept and droop controller. It is necessary to implement such control algorithms in a high penetration of solar power into the grid to maintain the stability of the system and operate along with conventional generators.

A dual inertia adaptive controller is used to calculate the virtual inertia constant based on the system dynamics in this paper. A comparative analysis is made in this paper to verify the effectiveness of the proposed dual adaptive controller. It is a decoupled methodology which makes a compromise between the frequency response and power output.

Keywords: Virtual synchronous generator, PV Inverter, battery energy storage, droop characteristics, frequency regulation.

INTRODUCTION

The rapid expansion of distributed generators (DGs) sources, such as photovoltaic, wind turbines, fuel cells, small and micro turbines, and others, gave rise to the microgrid concept. Inverters and other power-electronic devices are now used by most DGs to connect to the grid [1]. The virtual synchronous generator (VSG) control idea was developed because inverters' static nature prevents them from supporting the microgrid's frequency stability.

A VSG is a control method that enhances microgrid stability and control by enabling inverters to mimic the droop, damping, and inertial functions of synchronous generators (SGs) [2]. Researchers have put forth the VSG concept under a number of names, such as synchronverter [4] and virtual synchronous machine (VISMA) [3]. Furthermore, the VSG has been described in literature with other orders, such as second, third, fifth, and seventh order; nevertheless, the SG is often simulated using the second-order voltage source voltage-reference [5].

Although SGs have mostly been replaced by VSGs, certain SGs are still utilized in microgrids today. Most research simply assumes that because VSG shares characteristics with SGs, it may operate in parallel with them and effectively share the burden. Therefore, below we have tried to investigate this concept. This is accomplished by the study's detailed presentation of the VSG model and the parameter configuration for the paralleled VSG and SG. The VSG model is established for each unit. Parallel setups of VSG-VSG and SG-VSG are then used to compare the dynamic behavior of the VSG with the conventional SG in an isolated microgrid. The dynamic responses are compared using both proportional and equal sharing of the load demand.

To further improve the decoupling capabilities, many additional effective methods have been proposed, including the use of a communication network, a uniform rotation angle, and voltage correction. In [6], a decoupling method combining virtual inductive compensation and a voltage controller is proposed. Even though the voltage controller can compensate for voltage, it is difficult to pinpoint the exact value of the line impedance.

To adapt to low voltage microgrid coupling situations, a coordinated rotational transformation mechanism is proposed in [7]. However, the efficiency of this method relies on the exact value of the line impedance, which is difficult to ascertain. In [8], a method for controlling multi-variable-droop synchronous current converters is proposed. It enhances the current control loop with multivariable damping and synchronizing current. However, it might be challenging to configure each of the many exact parameters needed for excellent decoupling. In [9], an improved virtual power control method considering the unified rotation angle is proposed.

Since the degree of the link may be represented by the unified rotation angle, this method can effectively achieve decoupling. However, the method's potential to improve dynamic performance has been underutilized, and its separate process is a little complicated.

In [10], a decoupled control strategy that considers line impedance and load characteristics is proposed. Because the load might create power coupling, it is possible for the decoupled matrix to account for the influence of the load. However, figuring out the exact line impedance value is difficult, and changing the load characteristics could make the decoupling capabilities worse.

[11] proposes a virtual frequency and voltage frame to distinguish between active and reactive power. Since the virtual frequency and voltage in this way dictate the accuracy of power sharing, effective decoupling can be achieved by setting the proper parameters. However, as the frame transformation angle in the virtual frequency and voltage droop slopes differs for every DG unit, the fixed frame transformation angle can affect the decoupling's performance. [12] proposes a gain-scheduled decoupling control method that uses the extra control signals to achieve decoupling. However, the extra control signals may not be suitable for the dynamic system because they rely on the steady-state system's properties.

To accomplish exact power sharing, a distributed cooperative control-based droop control technique is put out in [13-16]. As a result, the system's performance is greatly enhanced. The inverter and microgrid are synchronized using a phase-locked loop (PLL). Through PQ regulation, the RES supplies the grid with steady real and reactive power. The components of the d-axis and q-axis AC currents are defined by the DQ reference frame, which is the basis for PQ control operation.

SYSTEM CONFIGURATION

The load is supplied by the system's two PV sources. To get the most power out of each PV array, a boost converter is employed. For each PV array, the rating is 4 kW at 300V DC. It uses a battery backup to power the important loads. The system's power supply determines when the battery is charged and discharged. A stand-alone system is examined in this research. The two PV inverters feed the load and run in parallel. To remove the harmonics, a 10kVAr capacitive filter is employed.

The droop and adaptive virtual inertia controller regulates each PV inverter's operation to lower the rate of change of frequency (RoCoF) when loads and faults vary. In a grid-connected system, the two inverters will provide both active and reactive power, which is essential for system stability.

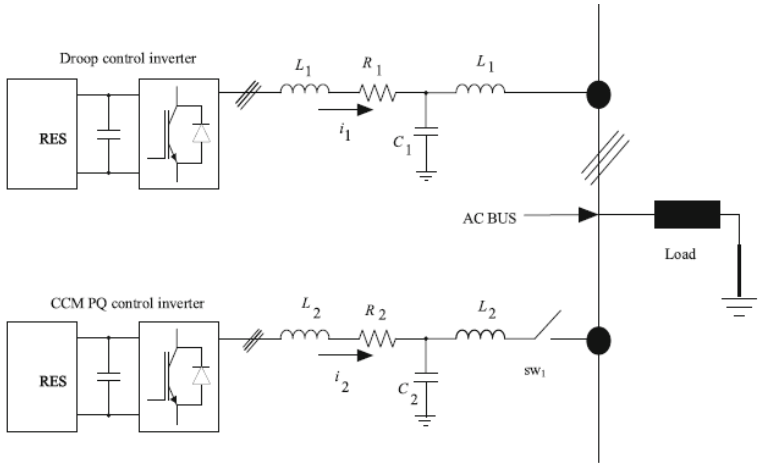

Figure 1. Block diagram of the system

2.1 Modelling of PV Source

An equivalent electrical circuit can be used to represent a photovoltaic cell. Typically, this circuit consists of a current source to represent the photocurrent, a diode to model the behavior of the p-n junction, a series resistance to account for connection losses, and a parallel resistance to represent leakage currents.

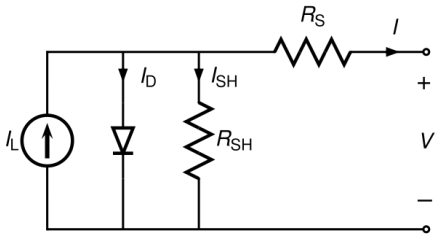

Figure 2. Equivalent circuit of PV Cell

$$I = I_L - I_0\left(e^{\frac{V+IR_S}{\eta V_t}} - 1\right) - \frac{V+IR_S}{R_{sh}} \quad (1)$$

I_{ph} = Photogenerated current (depends on irradiance and temperature)

I_s = Reverse saturation current; R_s = Series resistance

R_{sh}= Shunt resistance; V_t = Thermal voltage

n = Ideality factor: T = Temperature in Kelvin

k = Boltzmann's constant

A) Modelling of PV Inverter

To reduce the influence of the uncontrollable power coupling, coupling compensation is introduced into the traditional droop control strategy. And its formula is written:

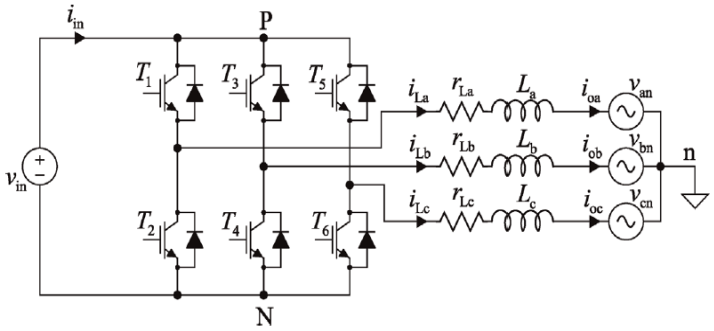

Figure 3. Modelling of PV Inverter

B) Design of Boost Converter

The basic structure and control topology of the boost converter is shown in Figure 4: This converter divides the dc-link into two levels: dc-link voltage at the output terminals of the diode rectifier, which is a variable dc voltage, and the dc-link voltage at the input terminals of the voltage source inverter, which is a constant voltage.

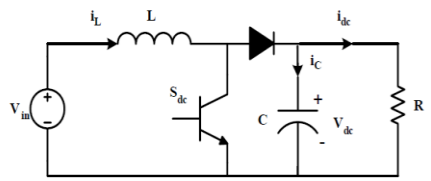

Figure 4. Boost converter for PV inverter

$$V_{out} = \frac{V_{in}}{1-D} \quad (2)$$

$$L_{min} = \frac{(1-D)V_{out}}{\Delta I_L f_s} \quad (3)$$

$$C_{min} = \frac{DI_{out}}{\Delta V_{out} f_s} \quad (4)$$

The duty cycle of the Boost converter is controlled to get the maximum power output from the PV array. P&O method is used to the maximum power output

CONTROL ALGORITHM

3.1 Droop Control Methodology

In a traditional alternator, the two synchronous generators exchange power using the droop control mechanism. Although the two PI inverters are run independently in this work as well, the power is divided based on their respective droop coefficients. These inverters rely solely on traditional generators to function. The upgraded droop controller's control block diagram is shown below.

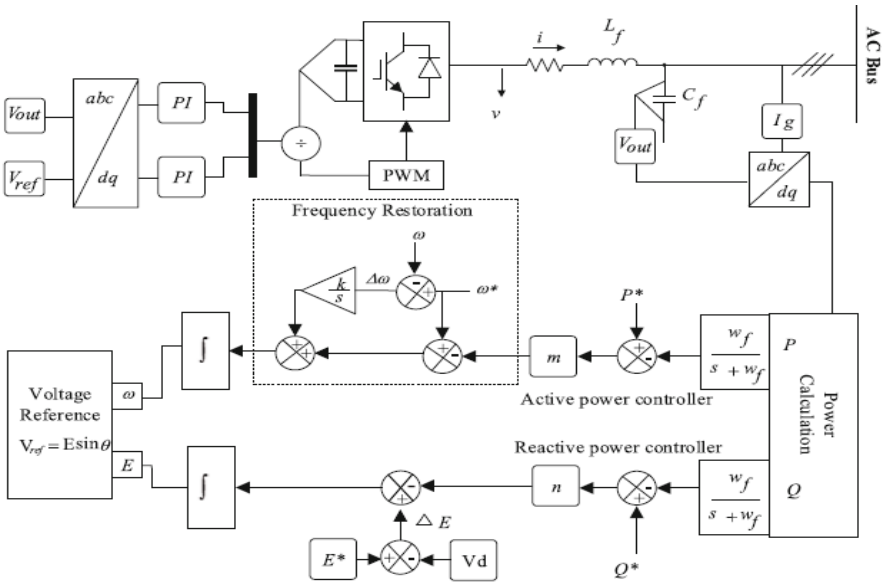

Figure 5. Enhanced Droop controller

3.2 Virtual Inertia Controller*:*

Grid-connected inverters use a Virtual Inertia Controller (VIC) to simulate the inertial response of conventional synchronous generators. By assisting with frequency management during abrupt load fluctuations or failures, this enhances grid stability. It is derived from the swing equation, which is provided by equation 3 below.

$$\omega = \omega N - m\,(P - Pref) \quad (4)$$

$$V = VN - n\,(Q - Qref) \quad (5)$$

$$2H\frac{d\omega}{dt} = \frac{d(\omega-\omega N)}{dt} = Pref - P0 - k((\omega - \omega grid) + 1/D\,(\omega\_ref - \omega grdi) \quad (5)$$

The image figure 6 below shows the control block diagram for the implementation of the virtual inertia controller used in this study. It may be difficult to calculate the value of the virtual inertia "H" at times. A higher virtual inertia value will cause the system to react more slowly.

Because of this, a lower H generates output active power that is dynamically better, responds more quickly, and oscillates less. larger inertia results in larger angular frequency changes even while it lessens power overshot. Consequently, this study builds an adaptive inertia controller in addition to the droop controller. This helps the PV inverter work more like a synchronous generator and enhances its frequency regulation capabilities.

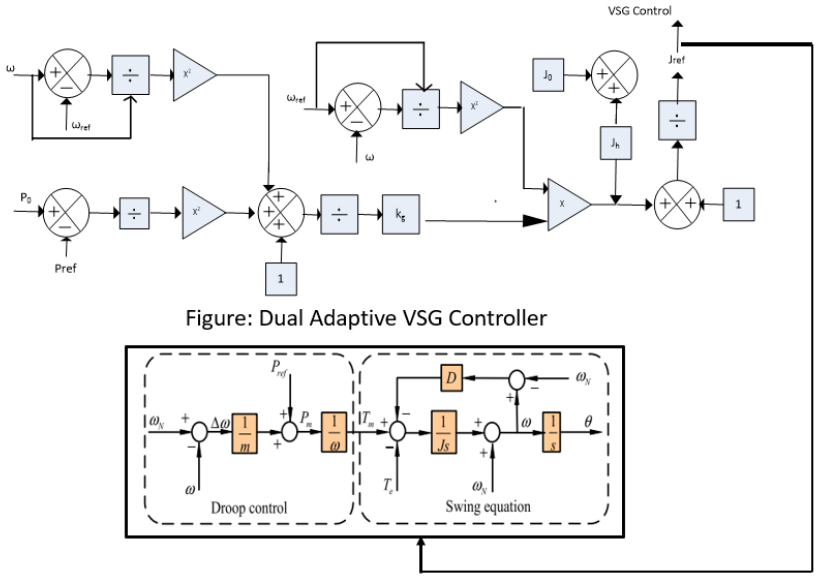

Figure: Dual Adaptive VSG Controller

Figure 6. Adaptive controller for Virtual Inertia controller

3.3 Overall Controller (Integration of Enhancing Droop Controller and Dual Adaptive Inertia Controller)

To replicate a conventional synchronous generator, the droop controller and the virtual inertia controller are combined. The droop controller will distribute power in accordance with the frequency ratings, while the virtual inertia controller, acting as a primary frequency controller, will use its inertia to mitigate the effects of sudden power changes. The frequency-dependent demands' fluctuation is controlled by the droop controller. Two PV inverters are operated by these integrated controllers, each of which performs frequency regulation. The control block diagram displays the entire control mechanism of two inverters connected in parallel. to increase the effectiveness of the frequency regulation as well.

SIMULATION RESULTS AND ANALYSIS

The following system parameters were taken into account when simulating the suggested system. Table 1 gives the various parameters. The insolation is varied and corresponding power is also varied from the two PV inverters

Table 1. System Parameters

S. No	Parameter	Rating
1	PV Array	4 kW, 300V
2	Boost converter	4.5 kW, 650V
3	Load	4kW, 1kVAR
5	Droop coefficient	m_1= 1% and m_2 = 1%
6	Virtual inertia	H1= 2sec and H2= 2sec
7	PV Filter	10 kVAr (Leading)
8	PWM	SPWM
9	f_{sw}	10 kHz

Initially the Solar inputs to the PV arrays are varied and the PV delivers the active power to the Boost converter. The following figure 6 and 7 shows the PV power output.

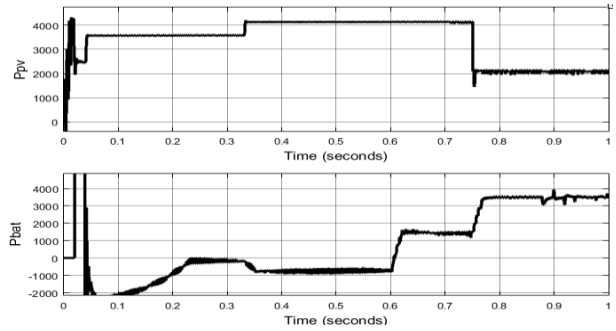

Figure 7. PV-1 and Battery output power

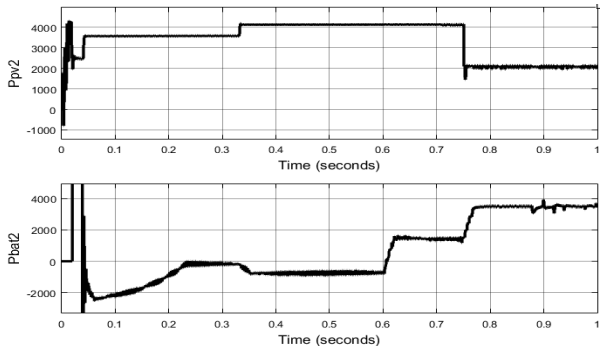

Figure 8. PV-2 power and its corresponding battery output power

In the above figure 8, the insolation is increased at t =0.35 seconds and decreased at to 0.75 seconds. With the increase in the PV power the battery is reduced at t= 0.35 seconds which is shown the above figure. The load is increased at t -0.6 sec as shown in the figure 9. With the increase in the load the battery power is varied accordingly to keep the system balance.

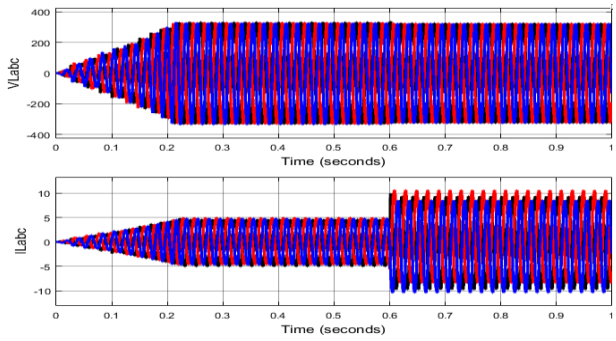

Figure 9. Load Voltage and Load current waveforms

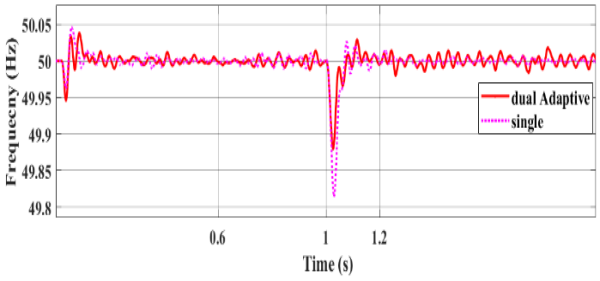

Figure 10. Frequency comparison of with dual adaptive and normal virtual inertia controller

In the figure 10, the frequency waveform is compared between the dual adaptive inertia controller and normal controller. It is observed that the dual adaptive controller the frequency dip is low compared to normal controller.

Figure 11 and 12 shows the power output waveforms of two inverters with different controllers. In the figure the no inertia waveform is obtained without any virtual inertia where as inertia 1 waveform is obtained only virtual inertia concept and it doesn't include the droop characteristics, while adaptive inerttia waveform is obtained considering dual adaptive and enhanced droop controller.

The frequency of the system is shown below figure 13. It is found that the with the droop controller and inertia controller the frequecny is reaching to 51 Hz, where as with the adajptive controller the increase in freqeucny is limited to 50.6 Hz. This shows the effectiveness of the integration of the enhanced droop controller as welll as adaptive inertia controller.

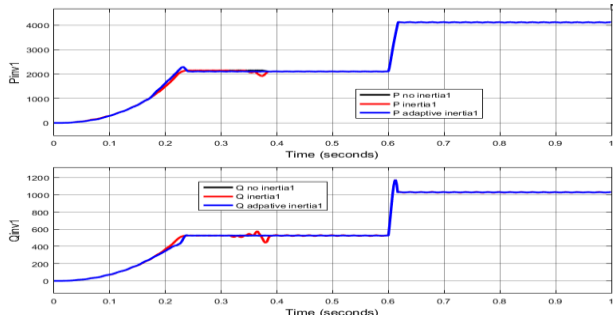

Figure 11. PV-1 Inverter output comparison with different controllers

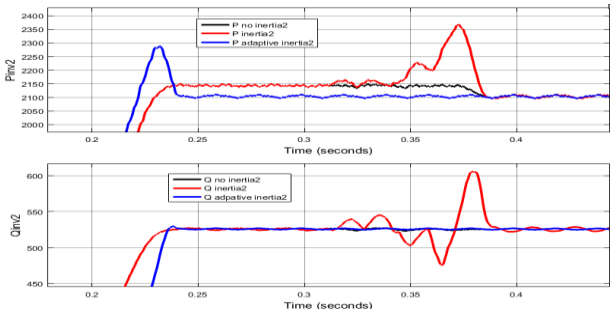

Figure 12. PV-2 Inverter output comparison with different controllers

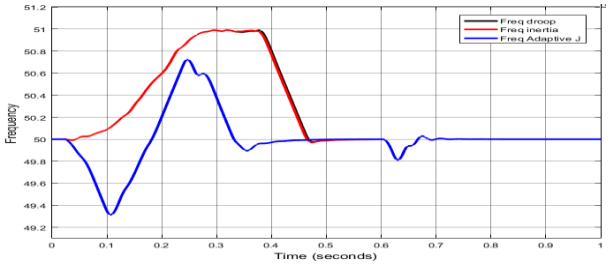

Figure 13. Comparative Frequency wave forms with different controllers

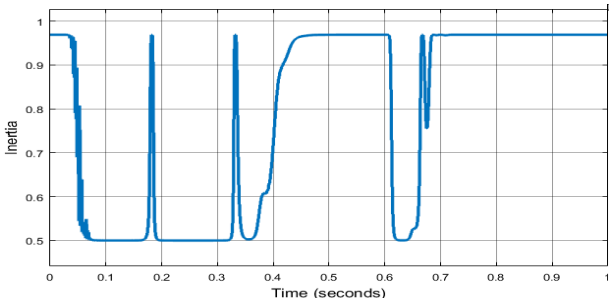

Figure 14. Virtual inertia value calculated based on the system parameters

REFERENCES

[1] U. Baader, M. Depenbrock, G. Gierse: Direct Self Control (DSC) of Inverter Fed Induction Machine: A Basis for Speed Control without Speed Measurement, IEEE Transaction on Industry Applications, Vol. 28, No. 3, May/June 1992, pp. 581 – 588.

[2] X. Hu, L. Zhang: A Predictive Direct Torque Control Scheme for a Three-level VSI-fed Induction Motor Drive, 9th International Conference on Electrical Machines and Drives, Canterbury, UK, 15 Oct. 1999, pp. 334 – 338.

[3] Hou, X., Han, H., Zhong, C., *et al.*: 'Improvement of transient stability in inverter-based AC microgrid via adaptive virtual inertia'. Energy Conversion Congress and Exposition (ECCE), Milwaukee, USA, September 2016, pp. 1–6.

[4] Van, T.V., Visscher, K., Diaz, J., *et al.*: 'Virtual synchronous generator: an element of future grids'. IEEE PES Innovative Smart Grid Technologies Conf. Europe (ISGT Europe),Gothenberg, Sweden, October 2010, pp. 1–7

[5] Beck, H.P., Hesse, R.: 'Virtual synchronous machine'. 9th Int. Conf. on Electrical Power Quality and Utilisation (EPQU), Barcelona, Spain, October 2007, pp. 1–6

[6] Zhong, Q.C., Weiss, G.: 'Synchronverters: inverters that mimic synchronous generators', *IEEE Trans. Ind. Electron.*, 2011, **58**, (4), pp. 1259–1267

[7] D'Arco, S., Suul, J.A.: 'Virtual synchronous machines—classification of implementations and analysis of equivalence to droop controllers for microgrids'. IEEE Grenoble InPowerTech (POWERTECH), Genoble, France, June 2013, pp. 1–7

[8] M. Kallamadi and V. Sarkar, "Enhanced real-time power balancing of an ac microgrid Through transiently coupled droop control," IET Generation, Transmission Distribution, vol. 11, no. 8, pp.1933–1942, 2017.

[9] P. Li, X. Wang, W. J. Lee, and D. Xu, "Dynamic power conditioning method of microgrid via adaptive inverse control," IEEE Transactions on Power Delivery, vol. 30, no. 2, pp. 906–913, April 2015.

[10] M. Ashabani, Y. A. R. I. Mohamed, M. Mirsalim, and M. Aghashabani,"Multivariable droop control of synchronous current converters in weak grids/microgrids with decoupled dq-axes currents," IEEE Transactions on Smart Grid, vol. 6, no. 4, pp. 1610–1620, Jul. 2015.

[11] T. Wu, Z. Liu, J. Liu, S. Wang, and Z. You, "A unified virtual power decoupling method for droop-controlled parallel inverters in microgrids," IEEE Transactions on Power Electronics, vol. 31, no. 8, pp. 5587–5603, Aug. 2016.

[12] X. Sun, Y. Tian, and Z. Chen, "Adaptive decoupled power control method for inverter connected dg," IET Renewable Power Generation, vol. 8, no. 2, pp. 171–182, March 2014.

[13] Y. Li and Y. W. Li, "Power management of inverter interfaced autonomous microgrid based on virtual frequency-voltage frame," IEEE Transactions on Smart Grid, vol. 2, no. 1, pp. 30–40, March 2011.

A. Haddadi, A. Yazdani, G. Jos, and B. Boulet, "A gain-scheduled decoupling control strategy for enhanced transient performance and stability of an islanded active distribution network," IEEE Transactions on Power Delivery, vol. 29, no. 2, pp. 560–569, Apr. 2014.

[14] J. Lai, H. Zhou, X. Lu, X. Yu, and W. Hu, "Droop-based distributed cooperative control for microgrids with time-varying delays," IEEE Transactions on Smart Grid, vol. 7, no. 4, pp. 1775–1789, Jul. 2016.

[15] Suleman Haider, Guojie Li and Keyou Wang, "A Dual control strategy for power sharing improvement in islanded mode of AC microgrid" Protection and Control of Modern Power Systems https://doi.org/10.1186/s41601-018-0084-2